

STATE-OF-THE-ART OF FOCUSED ION BEAM NANOLITHOGRAPHY

K. Arshak^{*}, M. Mihov^a

Electronic & Computer Engineering Dept., University of Limerick, Limerick, Ireland

^aMaterials & Surface Science Institute (MSSI), University of Limerick, Limerick, Ireland

Finely-focused ion beams can be applied for advanced lithography, which provides some advantages over conventional direct-write electron beam technology. In focused ion beam technology, however, the ion penetration depth is limited, thus requiring the use of extremely thin resist layers or higher ion acceleration energies. These requirements are often undesirable for the current IC manufacturing processes. One solution to this problem is to exploit the Top Surface Imaging (TSI) technique for dry developed FIB lithography schemes. In this paper, we investigate a novel lithography process, which combines focused Ga⁺ ion beam (Ga⁺ FIB) exposure, silylation and oxygen dry etching. The Negative Resist Image by Dry Etching (NERIME) is a TSI scheme for DNQ/novolac based resists, and can result in either positive or negative resist images depending on the extent of the ion beam exposure dose. The mechanism of negative image formation in NERIME is studied by TEM, and is found to be due to the creation of a thin gallium oxide layer during the oxygen dry development. Energy dispersive X-ray spectrometry microanalysis shows that gallium is implanted into the SPR660 resist to a depth of 50 nm and the oxidised gallium layer has a thickness of approximately 15 nm. It is also shown that the NERIME process can resolve nanometer resist patterns down to 65 nm, and yet maintain a high aspect ratio of 15. The NERIME process could be a useful nanofabrication method, as an alternative to the current lithography processes.

(Received December 9, 2004; accepted January 26, 2005)

Keywords: NERIME process, Nanolithography, Focused ion beams, Dry etching, TEM, EDS

1. Introduction

Semiconductor fabrication techniques are the key to major advances in the current complementary metal-oxide-semiconductor (CMOS) technology, and to realizing new functional quantum devices such as single electron transistors. Various nanofabrication techniques using photons, electrons and ions have been investigated over the last 20 years. Focused ion beam (FIB) technology is one of the most promising techniques for nanofabrication, because of its distinct advantage in being a maskless process and providing great flexibility and simplicity.

Since FIB technology was introduced into the semiconductor industry in the early 1980s, it has become a routine analytical tool for IC device analysis, circuit repair and advanced specimen preparation [1]. Nowadays, FIB tools are commonly used in the semiconductor, data storage and materials science industries. A FIB machine is very versatile, in that it can remove and deposit various types of material, including conductors and insulators, with sub-micron precision [2]. This function allows us to achieve tasks such as direct ion milling, chemical etching, ion implantation, and chemical deposition. Another important FIB function for the semiconductor industry is the ability to repair/modify IC circuits, in which the interconnects can be easily re-routed over specific chip areas by selective material removal and deposition. For example, the FIB method is used

* Corresponding author: khalil.arshak@ul.ie

routinely to repair optical binary masks for 193 nm lithography [3]. FIB tools have also found wide applications in secondary ion mass spectroscopy (SIMS) analysis.

2. FIB nanolithography and the NERIME process

The possibility of applying finely-focused ions for direct patterning lithography has been widely exploited in recent years. Three FIB methods have been studied in general for the nanofabrication of advanced IC devices, i.e. FIB direct milling, resist patterning with light ions, and dry development of FIB implanted resists [2,4,5].

2.1. Conventional FIB lithography

Conventional FIB lithography, as in the case of electron-beam exposure, can be used for direct photoresist patterning by using ions such as He^+ , Be^+ and Si^+ , followed by wet development [4]. This nanotechnology process can eliminate various problems associated with electron-beam lithography, such as low resist sensitivity and strong backscattering/proximity effects. The resolution of resist patterns exposed by ion beams is determined only by the lateral extent of the ion straggling distance. This is generally much smaller than that of scattered electrons in electron-beam lithography.

Some of the limitations for ion beam patterning technology, however, are connected with the limited penetration depth of light ions into the resist layer. At energies of 200 keV, for example, light ions of Be^+ and Si^+ penetrate into the PMMA resist down to depths of 1.2 μm and 0.6 μm , respectively [5]. By comparison, the much heavier Ga^+ ions used in FIB lithography can only penetrate the top 100 nm at 100 keV [6], which is not deep enough to expose the entire resist thickness. These restrictions significantly reduce the required resist thickness for conventional FIB lithography and, therefore, result in low aspect-ratio patterns, which are often inconvenient for the dry etching pattern transfer. As a solution to this problem, bilayer resist schemes for FIB lithography have been developed [5,6,7]. These schemes generally use a thin resist layer containing silicon, over a thick planarising layer. The top resist layer is exposed by FIB and wet developed, followed by transfer of the patterns to the bulk layer via an oxygen reactive ion etching (RIE) process. The regions where the silicon-containing resist layer remains are oxidized during the dry development, thus forming a silicon dioxide mask which protects the lower resist layer and results in positive image formation. Such a FIB bilayer resist method is capable of achieving nanometer resolution while maintaining a high aspect pattern ratio [6,7]. The drawback, however, is the use of the wet development step, which often results in resist swelling. This causes pattern deformation during the dry etching [4].

2.2. Dry developed FIB lithography

FIB lithography involving dry development can eliminate pattern deformation due to the swelling effects associated with the wet processing, and can thus yield high aspect ratio structures with nanometer resolution. FIB lithography can be combined with dry development processes using the well-known top surface imaging (TSI) technique [8]. The limited penetration range of the ions is a perfect match for the TSI processes, in which the surface of the resist is first covered with silicon-containing chemicals and then selectively exposed by an ion beam. These processes allow the unexposed area of the resist to withstand oxygen dry development. Other TSI processes utilize the dry development of ion-beam irradiated resist for negative image formation in the exposed area [5,9,10]. In the present study, some PMMA resist regions were implanted with different ion species such as Ga^+ and Si^+ . A significant reduction in the etching rates during the oxygen RIE process was indicated. The ion beam inhibited etching phenomenon can be explained in terms of the formation of stable oxide layers during the etching process, i.e. Ga_2O_3 and SiO_2 [5]. Another explanation of the etch resistance occurring in the implanted resist regions is the concept of physical hardening of the resist [10]. According to this interpretation, incident ions break the chemical bonds within the photoresist resin, by sputtering away both hydrogen and oxygen atoms. This results in the formation of a stable carbon-rich "graphitized" structure.

A novel scheme recently developed by the authors is the Negative Resist Image by Dry Etching (NERIME) process. This utilizes the same TSI and ion beam inhibited etching principles [11,12]. However, the main advantage of NERIME over similar FIB resist methods is its ability to produce both positive and negative patterns in a single resist layer process.

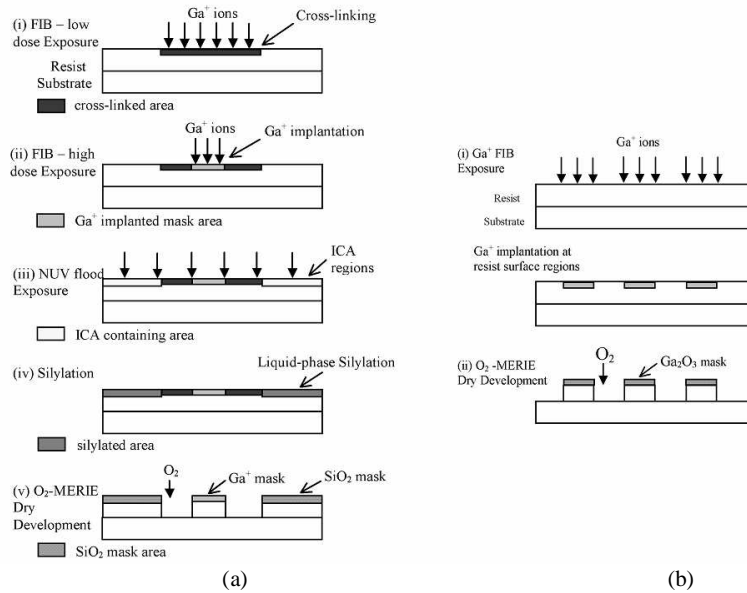


Fig. 1. (a) The NERIME process diagram and (b) the simplified two-step NERIME process.

The NERIME process consists of Ga^+ FIB exposure, near-ultraviolet (NUV) flood exposure, liquid-phase silylation, and oxygen RIE, as shown in Fig. 1(a). The process utilizes standard DNQ/novolak based resists, and involves two consecutive Ga^+ FIB exposures. The first of these is performed with a low-dose of Ga^+ ions. This chemically binds the photoactive compound with the novolak resin chains, thus promoting crosslinking in the exposed resist areas. The second Ga^+ exposure is carried out at much higher doses, which results in Ga implantation over the exposed resist regions. NUV flood exposure is then applied to convert the remaining PAC to indene carboxylic acid (ICA). In addition, the resist surface is treated with silicon-containing chemicals, which diffuse into the ICA-containing regions and cause a chemical reaction with the resin hydroxyl groups [11]. During the final oxygen RIE process, a thin protective SiO_2 layer is formed in the silylated regions, while the crosslinked resist region is etched away. Therefore, a positive resist image is formed in the exposed resist region by low-dose Ga^+ ions. The high-dose region, in which the Ga^+ ions are implanted, on the other hand, is believed to oxidize in a similar way to the silylated region and to form a Ga_2O_3 mask. As a result, these high-dose regions remain after the etching, and finally become negative images.

As seen in Fig. 1(b), the NERIME process can be further simplified to a negative-only resist scheme, by implementing two steps: a high-dose Ga^+ exposure and subsequent dry etching. The two-step NERIME, which uses the principle of ion beam inhibited etching, is a negative lithography process for DNQ/novolak-based resists. The resist region exposed to high Ga^+ doses in the two-step NERIME has a significantly lower etching rate in oxygen plasma than the unexposed region. As a result, such regions yield a negative resist pattern after etching.

3. Experimental procedure

A commercial I-line DNQ/novolak-based resist, Shipley SPR660, was used for the original NERIME and two-step NERIME experiments. A set of resist samples with different solvent concentrations was prepared: resist films 0.3 - 1.5 μm in thickness were obtained by spin-coating at 4000 rpm, followed by pre-baking at 90 $^\circ\text{C}$ for 60 sec on a hotplate. The Ga^+ ion exposures were carried out in a FEI FIB200 workstation operating at an accelerating voltage of 30 keV. Different exposure conditions were investigated using beam currents of 11, 70, and 150 pA. The exposure doses were calculated from the writing time, pattern area, and beam current. The NUV flood exposure was performed using a broadband Karl Suss MJB21 mask aligner, at a dose of 200 mJ/cm^2 . The liquid-phase silylation process was performed according to a procedure described in [13]. Dry-development was performed in a parallel-plate magnetically-enhanced reactive ion etching (MERIE) system, using oxygen plasma. The etching took place at 125 W RF power for a period of 400 - 1200

sec with an oxygen pressure of 0.05 - 5 mTorr. An axial magnetic field of 120 Gauss was applied during the etching process.

Transmission electron microscopy was performed using a FEI TECNAI 200F TEM/Scanning TEM (STEM) microscope, operating at an accelerating voltage of 200 keV. TEM specimens were prepared using the standard FIB trench and lift-out techniques. Care was taken to keep the temperature of the resist samples below 90 °C.

4. Results and discussion

The formation of negative images by both the original and the two-step NERIME process is governed by the mechanism of ion-beam inhibited etching. Our experimental steps involved exposing large resist areas to various doses of Ga^+ ions, followed by dry development of the exposed resist. Negative image formation occurred after the application of a relatively high exposure dose, in contrast to the positive image formation created by doses as low as $1 \mu\text{C}/\text{cm}^2$ [14]. Fig. 2 shows the sensitivity of the two-step NERIME process with SPR660 resist. It is evident that the critical dose of Ga^+ ions, required to form a negative image, must be higher than $800 \mu\text{C}/\text{cm}^2$ for 30 keV ion energies. This result is indeed consistent with the negative image formation in the original NERIME process [11]. Fig. 2 also shows results for a similar ion beam inhibited etching (IBIE) process, as reported in the literature [5] for negative patterning of PMMA photoresist by Ga^+ exposure and oxygen RIE. In the IBIE process, the ion beam exposure dose required to form a negative image was estimated to be in excess of $3000 \mu\text{C}/\text{cm}^2$.

An additional study of the ion beam inhibited etching effect in the NERIME process was carried out by TEM. Here, dry developed negative resist patterns with sub-micron dimensions were examined in a cross-sectional view. Fig. 3a shows a STEM micrograph of two $0.2 \mu\text{m}$ resist patterns produced by the NERIME process. The lines were exposed at a dose of $1.17 \times 10^{-2} \mu\text{C}/\text{cm}^2$ during the second Ga^+ exposure, and then dry-developed for 1200 sec at an oxygen pressure of 5 mTorr. To protect the resist surface from mechanical damage during TEM sample preparation, the surface was covered sequentially by thin gold and silicon dioxide layers. The dark gallium-enriched region is seen on top of the resist line in the bright field STEM image (Fig.3a). This dark contrast is due to the gallium-related mass absorption contrast created between the implanted and un-implanted resist areas. Images of the implanted resist regions were also taken using high-angle annular dark field (HAADF) STEM imaging, in which the image intensity increases with increasing atomic number (Fig. 3b). The gallium-enriched region, having a thickness of approximately 40 nm, appears brighter than the surrounding resist area.

In addition, a thin intermediate layer exhibiting slightly lower contrast is noticeable between the gold layer and the implanted gallium region. From the HAADF image, it can be concluded that this layer must contain a lower atomic element other than Ga. In view of probable Ga oxidation during the dry etching, we believe that the layer contains additional oxygen and, therefore, it is most likely to be the gallium oxide. The Ga_2O_3 layer was about 10 nm thick.

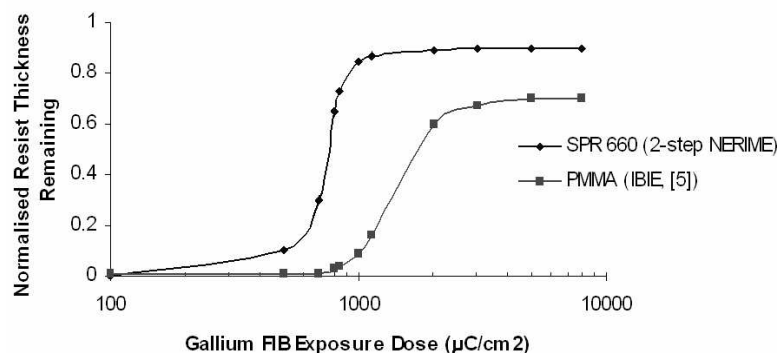


Fig. 2. Sensitivity of the two-step NERIME process using Shipley SPR660 resist. Results from a similar process scheme, IBIE [5], are shown, for comparison in the case of negative tone patterning of PMMA resist.

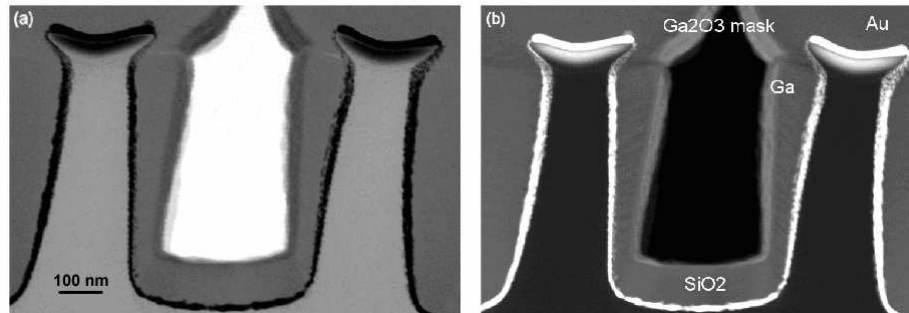


Fig. 3. (a) Cross-sectional bright-field STEM micrograph of two $0.2 \mu\text{m}$ negative resist lines produced by the NERIME process; (b) HAADF STEM micrograph of the same lines, showing the Ga implanted regions with a depth of 40 nm and the Ga_2O_3 mask layer with a thickness of approximately 10 nm .

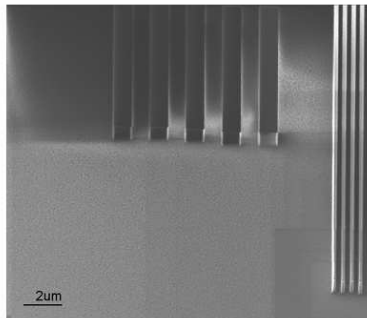


Fig. 4. FIB image of $1 \mu\text{m}$ and $0.1 \mu\text{m}$ lines/spaces in $1.5 \mu\text{m}$ thick SPR660 after the NERIME process. (Ga^+ beam doses of $5000 \mu\text{C}/\text{cm}^2$ and $2.5 \times 10^{-2} \text{ C}/\text{cm}^2$ respectively, 1000 sec MERIE at 0.05 mTorr).

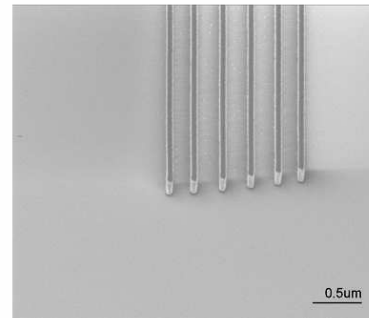


Fig. 5. FIB image of 80 nm lines in $0.3 \mu\text{m}$ SPR660 resist, produced by the NERIME process. (Ga^+ beam dose of $2 \times 10^{-2} \text{ C}/\text{cm}^2$, 400 sec MERIE at 0.05 mTorr).

The NERIME processes can achieve high resolution lithography on the nanometer scale by using relatively thick resist layers. This is due to the TSI concept of the image formation in NERIME, as well as the extremely small ion beam diameters down to 9 nm that are available on commercial FIB machines. Experiments were conducted by using a $1.5 \mu\text{m}$ thick resist, in which gratings of $1 \mu\text{m}$ and $0.1 \mu\text{m}$ resist lines/spaces were exposed to Ga^+ doses of 5000 and $2.5 \times 10^{-2} \text{ C}/\text{cm}^2$ respectively. Fig. 4 shows the dry developed profiles after 1000 sec of MERIE etching at an oxygen pressure of 0.05 mTorr . In comparison with the resist patterns in Fig. 3, the anisotropy of the developed patterns is clearly improved. This can be attributed to the reduced partial etching pressure, which led to a higher anisotropic etching by increasing the mean free path of oxygen ions. The developed patterns in Fig. 4 also demonstrated a very high aspect ratio of 15.

Additional NERIME experiments were carried out using a reduced resist thickness of $0.3 \mu\text{m}$, to resolve nanostructure patterns less than 100 nm . Fig. 5 shows 80 nm processed lines after the two-step NERIME process with a Ga^+ dose of $2 \times 10^{-2} \text{ C}/\text{cm}^2$ and MERIE dry-development for 400 sec at 0.05 mTorr . The NERIME patterns demonstrated the formation of well-defined vertical sidewalls with high anisotropy and minimal line-edge roughness. Smaller patterns with 65 nm width were also resolved at even lower exposure doses. Fig. 6 is an FIB image showing three different sets of NERIME resolved lines, obtained by exposure with Ga^+ doses of 8.15×10^{-3} , 1.2×10^{-2} and $1.6 \times 10^{-2} \text{ C}/\text{cm}^2$. The 65 nm resist lines remained after the MERIE etching.

The present results indicate that the NERIME process can be utilized for various nanotechnology applications, such as sub- 100 nm lithography for highly topographical surfaces that require thicker resist layers, and for lithography mask fabrication. To demonstrate the production of complex pattern layouts by the NERIME process, the University of Limerick logo was exposed by using an FEI pattern generator. Fig. 7 shows the dry developed image of this pattern, produced by exposing at an ion dose of $1.5 \times 10^{-2} \text{ C}/\text{cm}^2$ and dry-etching for 400 sec at 0.05 mTorr . The details of the imaged pattern are clearly resolved on the sub- 100 nm scale.

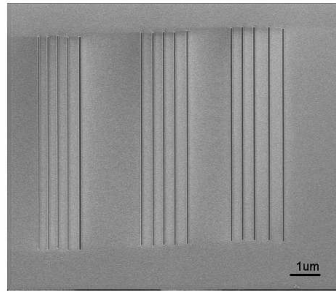


Fig. 6. FIB image of 65 nm lines in 0.3 μm SPR660, exposed at Ga^+ FIB doses of 8.15×10^{-3} , 1.2×10^{-2} and $1.6 \times 10^{-2} \text{ C/cm}^2$ respectively.

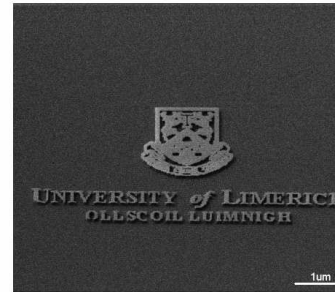


Fig. 7. FIB image of the University of Limerick logo, exposed at a Ga^+ FIB dose of $1.5 \times 10^{-2} \text{ C/cm}^2$ and dry developed for 400 sec at 0.05 mTorr.

4. Conclusions

New dry developed lithography methods were studied using a focused ion beam technique for nanotechnology applications. The Negative Resist Image by Dry Etching (NERIME) process combines Ga^+ FIB exposure and oxygen dry etching of single DNQ/novolac-based resist layers. Both positive and negative resist patterns can be obtained by varying the Ga^+ dose. In contrast to similar dry etching lithography methods reported in the literature, the two-step NERIME process offered higher resist sensitivity and better process contrast. A TEM analysis has revealed the presence of a thin gallium oxide layer on top of the gallium-exposed region. The gallium oxide layer was apparently formed during etching and is responsible for the negative image formation. The thickness of the gallium-implanted (an ion dose of $1.17 \times 10^2 \mu\text{C/cm}^2$ at 30 keV) resist regions was found to be approximately 40 nm. Various NERIME process conditions were also tested and optimized for nanolithography applications. Negative resist patterns with dimensions down to 65 nm were resolved by the NERIME process, which further demonstrated the formation of well-defined vertical resist sidewalls with minimal line-edge roughness and high aspect ratio.

References

- [1] J. Melngailis, *J. Vac. Sci. Technol.* **B5(2)**, 469 (1987).
- [2] R. Gerlach, M. Utlaut, *Proc. SPIE Charged Particles Detection, Diagnostics, and Imaging*, Vol. 4510, 2001, p.96.
- [3] D. Ferranti, A. Graupera, J. Marshman, D. Stewart, S. Szelag, *Proc. SPIE 23rd Annual BACUS Symposium on Photomask Technology*, Vol. 5256, p.546, 2003.
- [4] K. Gamo, *Microelectronics Engineering* **32**, 159 (1996).
- [5] H. Morimoto, Y. Sasaki, K. Saitoh, Y. Watakabe, T. Kato, *Microelectronics Engineering* **4**, 163 (1986).
- [6] S. Matsui, K. Mori, K. Saigo, T. Shiokawa, K. Toyoda, S. Namba, *J. Vac. Sci. Technol.* **B4(4)**, 845 (1986).
- [7] S. Matsui, Y. Kojima, Y. Ochiai, *Microelectronics Engineering* **11**, 427 (1990).
- [8] M. Harthey, D. Shaver, M. Shepard, J. Melngailis, V. Medvedev, W. Robinson, *J. Vac. Sci. Technol.* **B9(6)**, 3432 (1991).
- [9] H. Kuwano, *J. Appl. Phys.* **55(4)**, 1149 (1984).
- [10] I. Adesida, *Nuclear Instruments and Methods* **209-210**, 79 (1983).
- [11] K. Arshak, M. Mihov, D. Sutton, A. Arshak, S. B. Newcomb, *Microelectronic Engineering* **67-68**, 130 (2003).
- [12] K. Arshak, M. Mihov, A. Arshak, D. McDonagh, D. Sutton, S. B. Newcomb, *J. Vac. Sci. Technol.* **B22(1)**, 189 (2004).
- [13] K. Arshak, M. Mihov, A. Arshak, D. McDonagh, D. Sutton, S. Newcomb, T. J. Kinsella, *Proc. SPIE Opto Ireland 2002*, Vol.4876, 2003, p.525.
- [14] K. Arshak, M. Mihov, A. Arshak, D. McDonagh, D. Sutton, *Proc. 13 Int. Conf. on Photopolymers IBM RETEC 2003*, 2003, p46.